High-Resolution Imaging of the Self-Assembly of Organic Monolayers

Shirley Chiang

Organic monolayer films on surfaces have proven useful as chemical sensors, optical devices, and lubricants, among many other applications (*1*). In particular, alkanethiols with different functional groups have been studied in great detail in recent years because they self-assemble from solution into densely packed monolayer films on gold surfaces (*2*). These self-assembled monolayers (SAMs) are both easy to prepare and extremely stable. Many uses of these materials require manipulation of the surface molecular layer, so understanding the mechanism of their formation and ordering is extremely important. Although many techniques have been used to study the equilibrium structure of such layers, the mechanism of self-assembly of SAMs has been largely unknown until the work of Poirier and Pylant in this issue (*3*).

Their work was made possible by the scanning tunneling microscope (STM), which in recent years has allowed real-space imaging of individual molecules on metal surfaces (*4*). Poirier and Pylant (*3*) used an ultrahigh vacuum (UHV) STM to make high-resolution images of alkanethiols deposited from gas phase onto a clean Au(111) single crystal. These images provide a detailed molecular-scale picture of the mechanism of self-assembly of alkanethiols onto Au(111) and a direct observation of the nucleation, growth, and phase transitions of the molecular layers in real-time with molecular resolution. Poirier and Pylant suggest that the alkanethiol layer on Au(111) forms the following phases with increasing coverage: a lattice-gas phase, a low-density solid phase, and a higher density solid phase. The STM excels as a tool for examining structural changes in adsorbate layers as a function of coverage (*5*).

The Au(111) surface, which is the substrate for these studies, has a well-known uniaxial ($23 \times \sqrt{3}$) reconstruction (*6*) with alternating ordered domains forming a larger, ordered herringbone structure (*7*, *8*). Unlike Ni (*8*) or Fe (*9*), which grow on Au(111) at dislocations at the herringbone elbows, the alkanethiol molecules prefer to nucleate in large regions of unfaulted Au atom stacking, which occur in the ABC stacked regions between alternate herringbone elbows (*3*). The lattice-gas phase is not directly imaged by STM until the coverage is increased to the point that stable alkanethiol islands begin to nucleate. In the low-density solid phase ($solid_1$), the alkanethiol molecules form striped islands, which are elongated in the direction parallel to the hyperdomain ridges and have boundaries that conform to the herringbone turns. Interesting shapes occur in this phase (see figure): The elbows are compressed into denuded regions, and the striped-phase domains are oriented perpendicular to the preexisting hyperdomain ridges. Poirier and Pylant propose that these striped domains are comprised of alkanethiol molecules with the sulfur atoms bound in next-nearest neighbor threefold hollow sites with the molecular axes in the surface plane. These islands are also accompanied by dark depressions, which are islands of Au atom vacancies (*10*). At higher coverage, the high-density solid phase ($solid_2$) is characterized by elevated, corrugated islands that have a packing density identical to that of saturation coverage SAMs on Au(111), so that the molecular axes are now inferred to be along the surface normal for this phase.

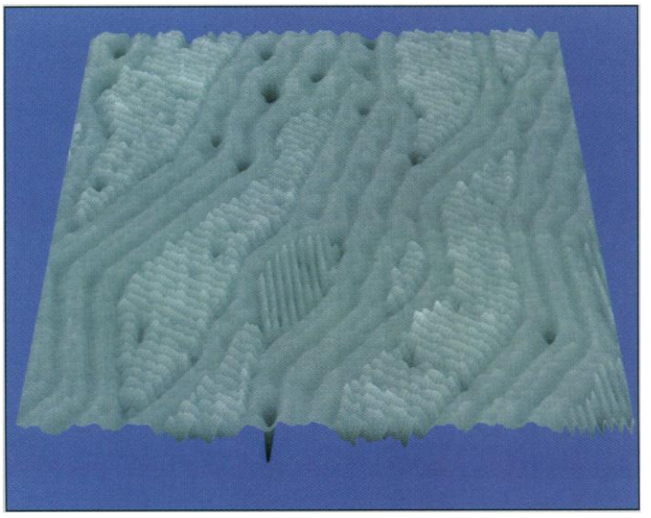

Intermediate stage of alkanethiol self-assembly on Au(111) surface as characterized by constant-current STM. Zigzag features are bare, reconstructed Au surface. Striped features are islands of alkanethiol molecules, arranged in rows, and with surface-aligned molecular axes. Dark depressions, such as in bottom center, are islands of Au atom vacancies.

High-resolution real-space STM images of nucleation and growth have often given unexpected results leading to surprising insights into the structure and growth of materials on a nanometer scale, compared with conclusions drawn from other techniques. Such examples abound in the field of metal-on-metal epitaxy, such as the nucleation of Ni or Fe at the herringbone elbows on Au(111). Other examples are the formation of islands of Au dendrites on Ru(0001) (*11*) and the growth of Pt on Pt(111), which forms a variety of island structures, ranging from compact dendritic structures to triangular islands, depending on the coverage and substrate temperature during deposition (*12*). Finally, remarkable insights into semiconductor epitaxy of Si (*13*) and Ge (*14*) on Si(100) and the cluster dynamics of growth have also been obtained with STM imaging.

For the alkanethiols on Au, the real-space imaging capabilities of the STM allow the different phases on the surface to be distinguished in the study of Poirier and Pylant (*3*). Judicious interpretation of the images then elucidated the mechanism of formation of the different phases. This study is the first in which such phases and their associated mechanism have been determined for a molecular adsorption system. Such work is also of fundamental interest because of its relation to two-dimensional phase transitions on surfaces.

As technology advances, the dimensions of the structures of interest grow steadily smaller. People now desire to manipulate nanometer-scale structures and even to design atomic- and molecular-scale arrays of ordered structures for information storage or small electrical circuits. In addition, it would be desirable to design materials to obtain specific physical or chemical properties. Thin molecular films could be an important constituent of such new materials, and thus, knowledge of both their structure and formation is important. Clearly, the STM is an extremely important tool for the understanding of molecular-scale structures and also possibly for the fabrication of such small structures.

The author is in the Department of Physics at the University of California, Davis, CA 95616, USA. E-mail: chiang@physics.ucdavis.edu

References

1. J. D. Swalen *et al.*, *Langmuir* **3**, 932 (1987).
2. L. H. Dubois and R. G. Nuzzo, *Annu. Rev. Phys. Chem.* **43**, 437 (1992).

3. G. E. Poirier and E. D. Pylant, *Science* **272**, 1145 (1996).
4. H. Ohtani, R. J. Wilson, S. Chiang, C. M. Mate, *Phys. Rev. Lett.* **60**, 2398 (1988).
5. K. E. Johnson, R. J. Wilson, S. Chiang, *ibid.* **71**, 1055 (1993).
6. U. Harten, A. M. Lahee, J. P. Toennies, Ch. Wöll, *ibid.* **54**, 2619 (1985); Ch. Wöll, S. Chiang, R. J. Wilson, P. H. Lippel, *Phys. Rev. B* **39**, 7988 (1989).
7. K. G. Huang *et al.*, *Phys. Rev. Lett.* **65**, 3313 (1990).
8. D. D. Chambliss, R. J. Wilson, S. Chiang, *ibid.* **66**, 1721 (1991).
9. B. Voigtländer, G. Meyer, N. M. Amer, *Surf. Sci.* **255**, L529 (1991); J. A. Stroscio, D. T. Pierce, R. A. Dragoset, P. N. First, *J. Vac. Sci. Technol. A* **10**, 1981 (1992).
10. O. Chilapakul, L. Sun, C. Xu, R. M. Crooks, *J. Am. Chem. Soc.* **115**, 12459 (1993); K. Edinger, A. Gölzhäuser, K. Demota, Ch. Wöll, M. Grunze, *Langmuir* **9**, 4 (1993).
11. R. Q. Hwang, J. Schröder, C. Günther, R. J. Behm, *Phys. Rev. Lett.* **67**, 3279 (1991).
12. M. Bott, T. Michely, G. Comsa, *Surf. Sci.* **272**, 161 (1992).
13. Y.-W. Mo *et al.*, *Phys. Rev. Lett.* **63**, 2393 (1989).
14. Y.-W. Mo, D. E. Savage, B. S. Swartzentruber, M. G. Lagally, *ibid.* **65**, 1020 (1990).

Viral Counts Count in HIV Infection

David D. Ho

When the acquired immunodeficiency syndrome (AIDS) first appeared, its pathogenesis was frustratingly elusive because the disease does not appear immediately upon infection with the human immunodeficiency virus (HIV). There is a variable period of time during which the patient remains healthy but exhibits viremia (the virus can be detected in the patient's blood). Recent work shows that this viremia is sustained by continuous rounds of viral replication and reinfection of blood cells (*1*, *2*), dispelling the notion that HIV has a true latent period. It follows that measuring the amount of virus in the blood (viral load) should be useful in determining the prognosis of the infected individual and in monitoring the effectiveness of therapies. Among a number of reports in support of this simple view is the elegant study in this issue by Mellors *et al.* (*3*), who show that a single measurement of plasma viral load can predict the subsequent risk of AIDS or death.

Since 1989, researchers have consistently shown that patients in advanced stages of HIV-1 infection have higher concentrations of virus in their blood (*4*). Moreover, the viral load after seroconversion (appearance of antibodies to HIV in the blood) predicts the likelihood of developing AIDS later (*5*). The authors of the new study (*3*) use a commercial amplification assay (*6*) to correlate the concentration of HIV-1 RNA in plasma with the clinical course of AIDS in a cohort of infected gay men, monitored since 1984. The findings are truly striking. For example, only 8% of patients with less than 4350 copies of RNA per milliliter of blood plasma progressed to AIDS 5 years after entering the study, whereas 62% of those with viral loads greater than 36,270 copies developed AIDS (see the figure). Individuals with intermediate viral loads had progression rates of 26 to 49%. A relative hazard of death of 1.55 was noted for each threefold increase in plasma viremia. Similar results have been observed in a recent study of infected hemophiliacs (*7*). The prognostic utility of measuring plasma viral load in HIV-1 infection is now unequivocal.

When HIV-1 enters a new host, there is typically a burst of viremia, which is then inhibited by the onset of immune responses (*8*) (see the figure). The subsequent level of plasma virus is a reflection of the equilibrium reached between the virus and the host after the initial battle and is generally maintained for years. This steady-state level varies from individual to individual and is predictive of the long-term clinical outcome (*3*, *5*, *7*).

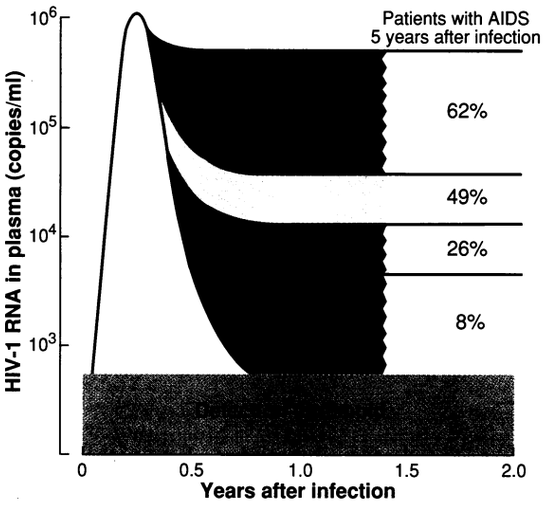

The course of HIV infection. Variable virologic setpoints after acute HIV-1 infection and their prognostic values. [Drawn from the data in (*3*)]

What does this virologic setpoint mean, and why is it so important prognostically? During steady state, HIV-1 clearance is balanced by its production, or $cV = \partial T^*N$ (*2*), where c is the rate constant for virion clearance, V is the virion concentration, N is the number of virions made per infected cell (burst size), T^* is the number of virus-producing cells, and ∂ is the rate constant for the loss of T^*.

Because the values for c and ∂ do not vary significantly among patients (*2*), $V \sim NT^*$, measuring the viral load yields clear information about the total number of productively infected cells and their average burst size. A static measurement of viral load provides a kinetic view of viral production, which in turn drives a fixed rate of CD4 lymphocyte destruction. Thus, it should not be surprising that viral load is a good surrogate marker for clinical outcome in HIV-1 infection. It is, indeed, a disease marker.

If high viral loads lead to poor clinical outcome, then lowering viral loads with antiviral drugs should result in improved prognosis. Does the evidence support this assertion? In several clinical trials of relatively weak antiretroviral regimens (*9*, *10*), consistent clinical benefits were observed in conjunction with modest reductions in plasma viremia. For example, in the AIDS Clinical Trials Group Protocol 175, a tenfold reduction in HIV-1 RNA concentration in plasma was associated with an ~50% decrease in the relative hazard of death (*10*). Recently, administration of a potent protease inhibitor, ritonavir, to patients in advanced stages of HIV-1 infection reduced viral loads by a factor of 3 to 16 for 16 weeks, which corresponded to ~45% lower risk of death (*11*). However, much more impressive antiviral effects are now regularly seen with certain combination therapies. One notable example is the use of indinavir, zidovudine, and lamivudine, which together reduced the viral load to less than 1%; indeed, 85% of these subjects had undetectable plasma viremia after 24 weeks of treatment (*12*). A decline in viremia of this magnitude should result in substantial clinical improvement (*3*, *7*, *9*–*11*), but the precise benefit awaits documentation. Nevertheless, many of the patients on potent combination therapies now have viral loads below those of long-term nonprogressors (*13*). Thus, if this dramatic suppression of HIV-1 is sustainable, these patients on combination treatment will present a unique opportunity to define the viral threshold below which disease progression does not occur. Imagine, as well, the future possibilities when addi-

The author is at the Aaron Diamond AIDS Research Center, The Rockefeller University, 455 First Avenue, New York, NY 10016, USA.